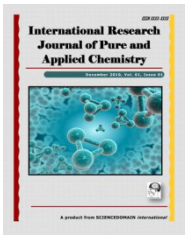

International Research Journal of Pure & Applied Chemistry
1(2): 30-41, 2011

SCIENCEDOMAIN *international*
www.sciencedomain.org

Sol-Gel Synthesis, Crystal Structure and Electronic Properties in $Bi_{2+x}Al_xNi_{4-3x}O_{7+\delta}$ ($0.0 \leq x \leq 0.75$) Composite Oxides

B. B. Das[1*] and M. Yogapriya[1]

[1]Department Materials Chemistry Laboratory, Department of Chemistry, Pondicherry University, Puducherry-605014, India.

Research Article

Received 1st May 2011
Accepted 15th May 2011
Online Ready 3rd June 2011

ABSTRACT

Sol-gel synthesis of $Bi_{2+x}Al_xNi_{4-3x}O_{7+\delta}$ (A1-A4: x = 0.0, 0.25, 0.50, 0.75) composite oxides were performed via nitrate-citrate route. Analysis of the powder XRD patterns by Fullprof shows cubic unit cell with lattice parameters in A1-A4: a = 10.2678, 10.1197, 10.1183, 10.1134 Å; Z= 4 and space group Pm3n. Average crystallite sizes in A1-A4 determined by Scherrer's relation are found to be in the range ~ 42-61 nm. The differential thermal analysis (DTA)/ thermogravimetric (TG) results show no phase transitions in the range 25-800 ºC. The morphology of the samples characterized by scanning electron microscopy (SEM) show similar results with respect to the particle sizes and shapes. Rietveld refinement of the unit cell structure shows appreciably lowered agreement factors R_p, R_{wp} and R_{exp} for all the samples. The Bi-O and Ni-O bonds of different sites show marginal variations in the samples. Circular electron density contours around Ni and O due to valence orbitals shows the partial ionic character of Ni-O bonds. The plane-wave Density Functional Theory (DFT) calculations on crystal of structure of A1-A4 for band structure and density of states (DOS) using a CASTEP programme package show the valence band (VB) located at -8.0 to ~ 0.0 eV (Fermi level) predominantly comprised of O 2p orbitals overlapping with in-phase with Ni t_{2g}, and the Bi 6s orbitals to form Ni-O-Bi bonds, and O 2p orbitals overlapping with Ni t_{2g} or Bi 6s forming O-Ni-O or Bi-O-Bi bonds. The conduction band (CB) is composed of Ni e_g orbitals, which narrows down with complete smearing of ~ 2.0 to 3.0 eV CB as in A1 in A2-A4 due to the absence of Al^{3+} d orbitals. This result shows the transition of semiconductor-like as in A1 to metallic character with the Ni e_g band predominantly crossing the Fermi level, in A2-A4.

**Corresponding author: Email: das_b_b@yahoo.com;*

Keywords: Sol-gel synthesis; composite oxides; powder xrd; Rietveld refinement; DFT calculations; electronic energy bands; density of states;

1. INTRODUCTION

In the past decade, the preparation and characterization of new composite oxide materials have become a topic of great interest, both experimentally and theoretically. Transition metal oxides, because of the interesting diverse physical properties they exhibit, relatively easy to prepare, and low cost, have attracted much attention as the new materials in recent years. The study of physical properties of composite oxides requires single-phase samples because electrical transport and magnetic properties are closely related to the structure. Therefore, it is necessary to ensure if the samples are really monophasic. Of special interest to us are the novel hybrid metal-ceramic materials prepared by sol-gel technique (Roy and Roy, 1984). This technique has enabled the preparation of variety of interesting solid materials including composite oxides, ceramic powders and glasses (Roy and Roy, 1984; Komarneni et al.,1986). Located at the center of the first transition metal series, Ni^{2+} is a good trap of photogenerated hole converting it to Ni^{3+}, which is good oxidant of organic molecule through formation of carbocataion (Ghorai et al., 2008). The holes associated with a quadrupole complex contribute to conductivity by hopping and/or by band like conduction, depending on various parameters like temperature, frequency of the applied signal, defect concentration, and dopant concentration, if any (Morin, 1954). The nature of the highest occupied bands, responsible for the electronic properties of a material, is strongly dependent on both its composition and its crystal structure. In this present study, we report on the synthesis of new series of composite oxides materials, $Bi_{2+x}Al_xNi_{4-3x}O_{7+\delta}$ (x = 0.0, 0.25, 0.5, 0.75) by sol-gel method via nitrate-citrate route, detailed analysis of crystal structure and calculations of the electronic energy band structure and density of states (DOS) by the plane-wave-density functional theory (DFT). The substitution effects of the trivalent cations M^{3+} (Bi^{3+} and Al^{3+}) on the electronic structure are also studied.

2. MATERIALS AND METHODS

2.1 Sample Preparation

Synthesis of $Bi_{2+x}Al_xNi_{4-3x}O_{7+\delta}$ (A1-A4: x = 0.0, 0.25, 0.50, 0.75) composite oxides was performed by sol-gel method via nitrate-citrate precursor route. Calculated amounts of stoichiometric bismuth nitrate, $Bi(NO_3)_3{\cdot}5H_2O$, aluminium nitrate, $Al(NO_3)_3$ and nickel nitrate, $Ni(NO_3)_2$, were dissolved in acidified (HNO_3) water to prepare a solution of pH ~ 2 each. The solutions were mixed together and stirred for 1 h at ~ 50 ˚C, then ~30 ml 1.5 M solution of citric acid was added and stirred continuously ~ 50 ˚C for ~ 90 h which then forms a waxy gel. The resulting gel was then decomposed at ~ 120 °C, which was then sintered in air successively at 450 ºC for 2 h for complete combustion of organic materials, and at 800° C for 4 h and quenched in air to obtain fine green powder.

2.2 Experimental Techniques

The powder X-ray diffraction (XRD) pattern of the samples were recorded on an X'pert powder X-ray diffractometer (PAN ANALYTICAL make) with scan rate 2°/ minute in range 5° - 75° in 2θ. Monochromatic Cu K_α radiation (λ ~ 1.5418 Å) was used as the x-ray source with power 40 kV/30 mA. The powder x-ray diffraction data were analyzed by the FullProf Suite (version 3.90) software package (Carjaval, 1990) to determine the unit cell parameters and indexing. The refinement of the unit cell structure was done using Rietveld refinement method (McCusker et al., 1999). The Fourier electron density mapping on the crystal structure after refinement was done using FullProf Suite (version 3.90) software. The microstructures of the samples were examined by a SEM JSM-5410, and the distribution of the elements throughout the grains and the chemical compositions of the samples were determined from the EDX profiles recorded using a Hitchi-S3400 instrument. DTA/TG analysis was done using a Perkin-Elmer Diamond TG/DTA instrument (sensitivity of 0.2 μg) in the range 25- 800 °C at heating rate of 25°C/min in air. The densities of the samples are determined by liquid displacement method using carbon tetrachloride as a immersion liquid (density 1.596 g/cc at 300 K).

2.3 Band Structure and Density of States Calculations

The calculations of electronic energy band structures and density of states were done using a plane-wave density functional theory with local gradient-corrected exchange-correlation functional (Perdew et al., 1996) and performed with a commercial version of the CASTEP (Cambridge Serial Total Energy Package) programme package, (Clark et al., 2005; Segall et al., 2002a,b; Payne et al.,1992) using Material Studio (MS) software which uses a plane-wave basis set for the valence electrons and norm-conserving pseudopotential (Hamman et al., 1979) for the core states.

3. RESULTS AND DISCUSSION

3.1 Determination of Unit Cell Parameters

The powder XRD patterns of samples A1-A4 of $Bi_{2+x}Al_xNi_{4-3x}O_{7+\delta}$ ($0.0 \le x \le 0.75$) composite oxide system are shown in Figure 1. Using the Fullprof software the unit cell parameters as well as the indexing of the lattice planes in the samples A1-A4 are done. The unit cell in the samples is found to be cubic with space group Pm3n. The cell parameters are shown in Table 1 along with the observed densities of the samples. Comparison of the observed density with the calculated ones show that Z=4 for the samples A1-A4. The cell dimension decreases in A1-A4 with increasing x. This is attributed to the incorporation of higher valent Bi^{3+} and Al^{3+} ions in the lattice. The average crystallite sizes in the samples are determined by Scherrer's relation (Klug and Alexander, 1997), and the values are also shown in Table 1. The crystallite sizes are in the plausible range of 42-61 nm in the samples.

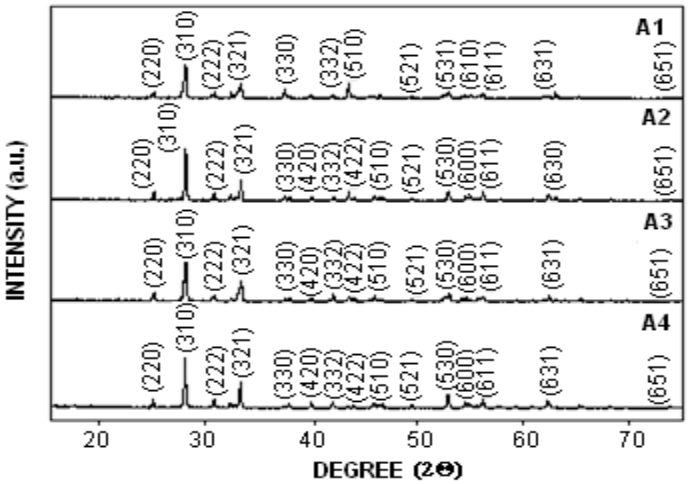

Fig. 1. Powder XRD patterns and indexed lattice planes of A1-A4 of $Bi_{2+x}Al_xNi_{4-3x}O_{7+\delta}$ (0.0 ≤x≤ 0.75) composite oxides

Table 1. Unit cell parameters, calculated and observed densities and average crystallite sizes in A1-A4 of $Bi_{2+x}Al_xNi_{4-3x}O_{7+\delta}$ (0.0 ≤ x ≤ 0.75) composite oxides

Unit cell data/Sample	A1	A2	A3	A4
Cell Formula	$Bi_8Ni_{16}O_{28}$	$Bi_9Al_1Ni_{13}O_{28}$	$Bi_{10}Al_2\ Ni_{10}\ O_{28}$	$Bi_{11}Al_3Ni_7O_{28}$
Lattice parameter* a (Å)	10.2767	10.1197	10.1183	10.1134
Cell volume (Å^3)	1085.32	11036.35	1035.90	1034.40
Space group	Pm3n	Pm3n	Pm3n	Pm3n
Z	4	4	4	4
Calculated density (g/cc)	4.693	4.944	5.013	5.065
Experimental density (g/cc)	4.398	4.946	5.169	4.825
Average crystallite size (nm)	42	50	45	61

** before refinement*

3.2 Microstructure, EDX and Thermal Studies

Figure 2 shows the SEM micrographs A1 and A4, and EDX profile of representative sample A4. The high magnification SEM micrograph of A4 is shown in the inset in Figure 2(b), which shows particles with quadrupods-like shape with random orientations. Investigation of various regions of the sample also shows similar results with respect to the particle sizes and shapes. The compositions of the samples were characterized by EDX profiles which show that all samples have the stoichiometry close to nominal. The EDX analysis indicated homogeneous distribution of all elements, within the grains of the samples. The mapping of

the samples also shows the high dispersion and homogeneity in distribution of elements in the samples.

DTA and TG traces show no endothermic peak with weight loss upto 600 ºC indicating no absorption of moisture or co-ordinated water in the samples. Rather the weight increase in TG curve in the range 20-400 °C (~1.2 %) may be resulted from the oxidation of the nickel present in the system. DTA curves show an endothermic peak with weight loss at 630 ºC. No other anomalies were observed. This fact indicated that no any phase transitions upto 800ºC.

3.3 Crystal Structure Refinement and Electron Density Fourier Mapping

The unit cell structure (Figure 3(a)-(b)) of the samples A1-A4 is developed on space group Pm3n (sp. gr. No. 223) with Z=4. The Bi^{3+} ions are put in 8(e) sites in A1 with additional Bi^{3+} ions in A2-A4 in 6(d) sites; Ni^{2+}(or Al^{3+}) ions in 12(f) and 6(c) sites; O^{2-} ions in 16(i) and 12 (f) sites. The unit lattice dimensions and the agreement factors after Rietveld structure refinement (McCusker et al., 1999) are shown in Table 2. The Tables 3-5 also show the refined atomic position coordinates, bond lengths and bond angles in the asymmetric units of A1-A4, respectively.

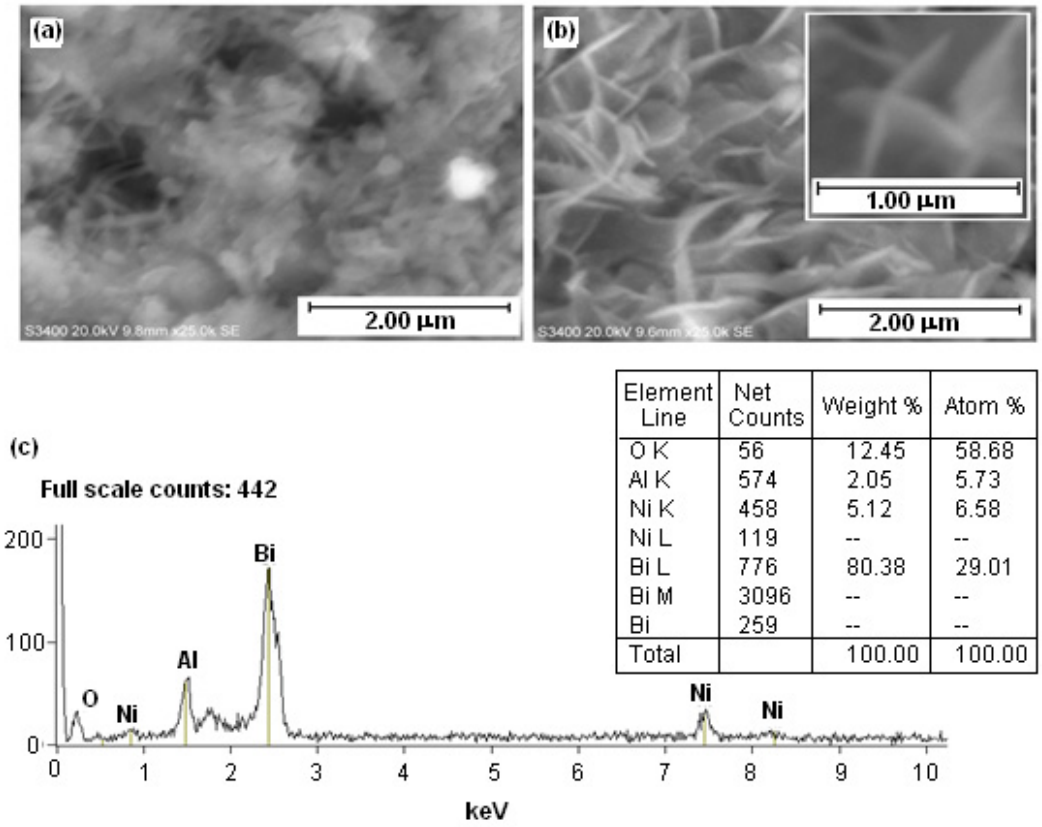

Element Line	Net Counts	Weight %	Atom %
O K	56	12.45	58.68
Al K	574	2.05	5.73
Ni K	458	5.12	6.58
Ni L	119	--	--
Bi L	776	80.38	29.01
Bi M	3096	--	--
Bi	259	--	--
Total		100.00	100.00

Fig. 2. (a) SEM micrographs of A1, and (b) SEM micrographs of A4 at different magnifications (c) EDX profiles of A4 with compositions of the elements in randomly selected grain (inset).

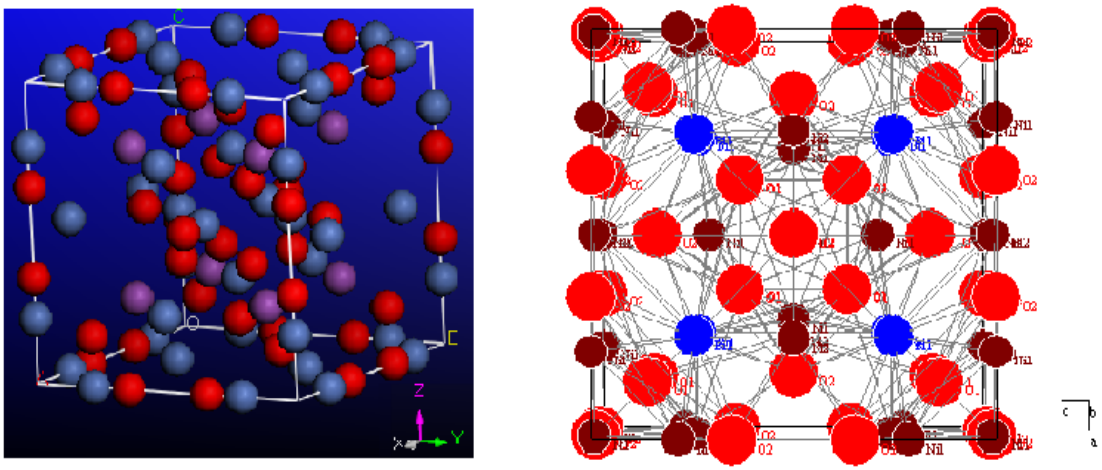

(a) (b)

Fig. 3. (a) 3-dimensional, and (b) 2-dimensional view on (001) plane of $Bi_8Ni_{16}O_{28}$ (A1: x=0.0) unit cell structure. Bi-dark red, Ni(Al)-blue, O-red in 2-dimensional view

Table 2. Unit cell dimension, a (Å), and the agreement factors after Rietveld refinement of the unit cell structure of A1-A4 of $Bi_{2+x}Al_xNi_{4-3x}O_{7+\delta}$

Agreement Factors	Samples			
	A1	A2	A3	A4
a (Å)	10.2678	10.1266	10.1160	10.1163
R_p (%)	97.10	96.19	96.14	95.97
R_{wp} (%)	99.83	96.80	96.98	96.37
R_{exp}(%)	0.23	0.26	0.30	0.23

At first sight, it appears that for the compositions A2-A4, no significant changes are observed in the bond lengths suggesting that the total bonding interaction is practically constant in the composition range studied. No significant change in bond angles is also observed in the samples. This is related to the microstructure of the samples which show uniform behaviour. The Fourier mapping of the 3-dimensional electron density from xz-plane (010), and the 2-dimensional electron density contour on (010) plane are shown in Figures 4(a)-(b), respectively. The circular nature of the contours around the Ni due to localized valence d orbitals and the O due to valence 2s and 2p orbitals in the lattice sites with isolated overlapping contours also shows the partial ionic character of Ni-O bonds (Hugel and Carabatos, 1983) in the crystal.

Table 3. Generated crystal coordinates (xyz) and Cartesian coordinates (XYZ) before and after refinement of the atomic positions in the asymmetric unit in A1-A4 of $Bi_{2+x}Al_xNi_{4-3x}O_{7+\delta}$ ($0.0 \le x \le 0.75$) composite oxides

Sample/ No	Atom	Crystal coordinates			Cartesian coordinates before refinement			Cartesian coordinates after refinement		
		x	y	z	X	Y	Z	X	Y	Z
A1										
1	Bi1	0.2500	0.2500	0.2500	-2.5669	-2.5669	-2.5669	-2.5670	-2.5670	-2.5670
2	Ni1	0.7853	0.0000	0.0000	2.9293	-5.1338	-5.1338	2.9293	-5.1339	-5.1339
3	Ni2	0.2500	0.0000	0.5000	-2.5669	-5.1338	0.0000	-2.5670	-5.1339	0.0000
4	O1	0.1363	0.1363	0.1363	-3.7344	-3.7344	-3.7343	-3.7345	-3.7344	-3.7344
5	O2	0.6501	0.0000	0.0000	1.5411	-5.1338	-5.1338	1.5411	-5.1339	-5.1339
A2										
1	Bi1	0.2500	0.2500	0.2500	-2.5300	-2.5299	-2.5299	-2.5317	-2.5317	-2.5317
2	Bi2	0.2500	0.5000	0.0000	-2.5300	0.0000	-5.0599	-2.5317	0.0000	-5.0633
3	Ni1	0.7853	0.0000	0.0000	2.8871	-5.0599	-5.0599	2.8890	-5.0633	-5.0633
4	Ni2	0.2500	0.0000	0.5000	-2.5300	-5.0599	0.0000	-2.5317	-5.0633	0.0000
5	O1	0.1363	0.1363	0.1363	-3.6806	-3.6806	-3.6805	-3.6831	-3.6831	-3.6830
6	O2	0.6501	0.0000	0.0000	1.5189	-5.0599	-5.0599	1.5199	-5.0633	-5.0633
A3										
1	Bi1	0.2500	0.2500	0.2500	-2.5296	-2.5296	-2.5296	-2.5290	-2.5290	-2.5290
2	Bi2	0.2500	0.5000	0.0000	-2.5296	0.0000	-5.0592	-2.5290	0.0000	-5.0580
3	Ni1	0.7853	0.0000	0.0000	2.8867	-5.0592	-5.0592	2.8860	-5.0580	-5.0580
4	Ni2	0.2500	0.0000	0.5000	-2.5296	-5.0592	0.0000	-2.5290	-5.0580	0.0000
5	O1	0.1363	0.1363	0.1363	-3.6801	-3.6801	-3.6800	-3.6793	-3.6792	-3.6792
6	O2	0.6501	0.0000	0.0000	1.5187	-5.0592	-5.0592	1.5183	-5.0580	-5.0580
A4										
1	Bi1	0.2500	0.2500	0.2500	-2.5284	-2.5284	-2.5284	-2.5291	-2.5291	-2.5291
2	Bi2	0.2500	0.5000	0.0000	-2.5284	0.0000	-5.0567	-2.5291	0.0000	-5.0581
3	Ni1	0.7853	0.0000	0.0000	2.8853	-5.0567	-5.0567	2.8861	-5.0582	-5.0581
4	Ni2	0.2500	0.0000	0.5000	-2.5284	-5.0567	0.0000	-2.5291	-5.0581	0.0000
5	O1	0.1363	0.1363	0.1363	-3.6783	-3.6783	-3.6782	-3.6794	-3.6793	-3.6793
6	O2	0.6501	0.0000	0.0000	1.5179	-5.0567	-5.0567	1.5184	-5.0582	-5.0581

Table 4. Bond lengths (Å) in asymmetric units of A1-A4 of $Bi_{2+x}Al_xNi_{4-3x}O_{7+\delta}$ ($0.0 \le x \le 0.75$) composite oxides

S.No.	Atoms	A1	A2	A3	A4
1	Bi1-O1	2.0221 (16)	1.9943 (16)	1.9922 (16)	1.9923 (16)
2	Bi2-O1	--	4.0982 (48)	4.0940 (48)	4.0941 (48)
3	Ni1-O1	2.1367 (48)	2.1073 (48)	2.1051 (48)	2.1051 (48)
4	Ni1-O2	1.3882 (30)	1.3691 (30)	1.3677 (30)	1.3677 (30)
5	Ni2-O1	4.1554 (48)	4.0982 (48)	4.0940 (48)	4.0941 (48)
6	Ni2-O2	6.5752 (24)	6.4848 (24)	6.4780 (24)	6.4782 (24)

Table 5. Bond angles in degrees in asymmetric units of A1-A4 of $Bi_{2+x}Al_xNi_{4-3x}O_{7+\delta}$ ($0.0 \leq x \leq 0.75$) composite oxides

Sl. No.	Atoms	A1	A2	A3	A4
1	Bi1-O1-Bi2	--	60.8813 (1)	60.8813 (24)	60.8813 (1)
2	Bi1-O1-Ni2	60.8813 (1)	60.8813 (1)	60.8813 (24)	60.8813 (1)
3	Bi2-O1-Ni2	--	121.7626 (1)	121.7626 (45)	121.7626 (1)
4	Ni1-O2-Ni2	128.6665 (1)	128.6665 (1)	128.6665 (20)	128.6665 (1)
5	O1-Ni2-O2	58.2540 (1)	58.2540 (1)	58.2540 (24)	58.2540 (1)

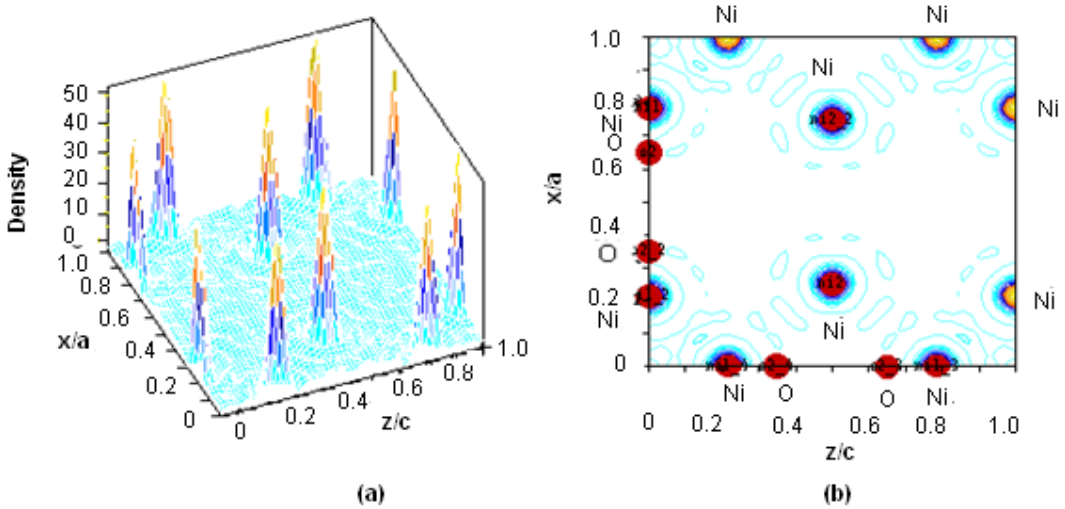

Fig. 4. (a) 3-dimensional electron density from (010) plane, (b) 2-dimensional electron density contour on (010) plane of $Bi_8Ni_{16}O_{28}$ (A1) showing the symmetric positions of Ni and O atoms on the plane.

3.4 Band Structure and Density of States

The Figures 5(a)-(b) and Figures 5(c)-(d) show the electronic energy band structures and the density of states, of representative samples A1 and A4, respectively, calculated by the plane-wave density functional theory method using a commercial version of the CASTEP programme package. This program evaluates the total energy of periodically repeating geometries based on density-functional theory and the pseudopotential approximation. In this case only the valence electrons of the elements are represented explicitly in the calculations, and the valence-core interaction being described by nonlocal pseudopotentials. The band structure of the composite oxides predominantly having MO_6 (M=transition metal) polyhedra may be represented by the transition metal d and the O 2p orbitals (Li et al., 2006). Figure 6 shows the calculated total density of states and partial density of states of elements O, Ni, Al, and Bi in $Bi_{11}Al_3Ni_7O_{28}$ (A4: x= 0.75). The Fermi level is pinned at 0 eV. A smearing of 0.5 eV is used to generate the DOS plots. It can be seen that the samples do not have clear band gap. Four occupied bands and one unoccupied band are visible from the density of states diagrams, in which the bands consists of O 2s and Al 2s, Bi 6s, O 2p, Ni

3d and Al 2p orbitals in turn form the lowest to the highest bands. The band located at -8.0 to +1.0 eV is due to O 2p orbitals (Li et al., 2006), the band located at -8.0 to +0.5 eV is due to Bi 6s orbitals (Zhou et al., 2007), and the band at -8.0 to +1.0 eV is due to the Ni 3d orbitals (Wei et al., 2010). Due to the overlapping of Ni 3d and O 2p orbitals it is reasonable to assume that Ni d orbitals will be split into t_{2g} and e_g under the preferable octahedral field on composite oxide matrices. This means that O 2p orbitals overlap in phase with Ni t_{2g} and the Bi 6s orbitals to form Ni-O-Bi bonds, or O 2p orbitals may overlap with Ni t_{2g} or Bi 6s forming O-Ni-O or Bi-O-Bi covalent bonds with partial ionic character, which comprises the valence bands (VB). Formation of Ni-O-Bi or O-Ni-O bonds in the samples is evidenced by the powder XRD analysis by Rietveld refinement (McCusker et al., 1999) of crystal structures of the samples discussed earlier.

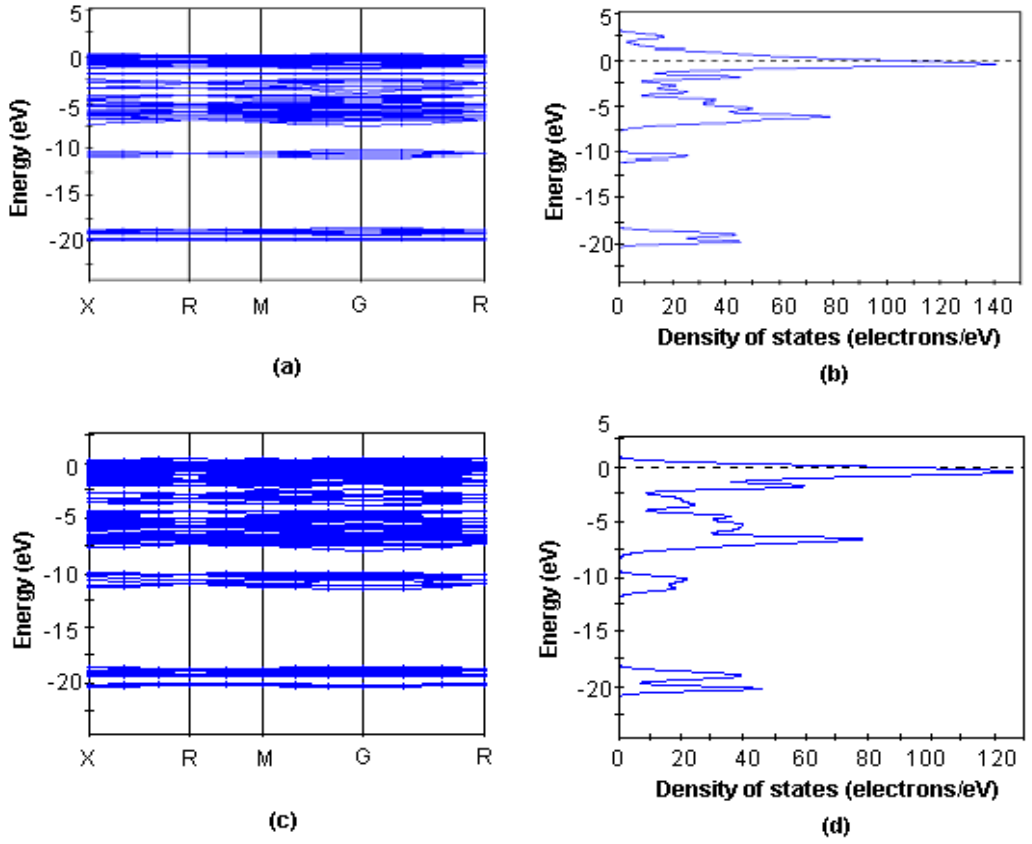

Fig. 5. (a) Band structure and (b) density of states of $Bi_8Ni_{16}O_{28}$(A1); and (c) band structure and (d) density of states for $Bi_{11}Al_3Ni_7O_{28}$ (A4) calculated using a plane-wave density functional theory with a CASTEP programme package

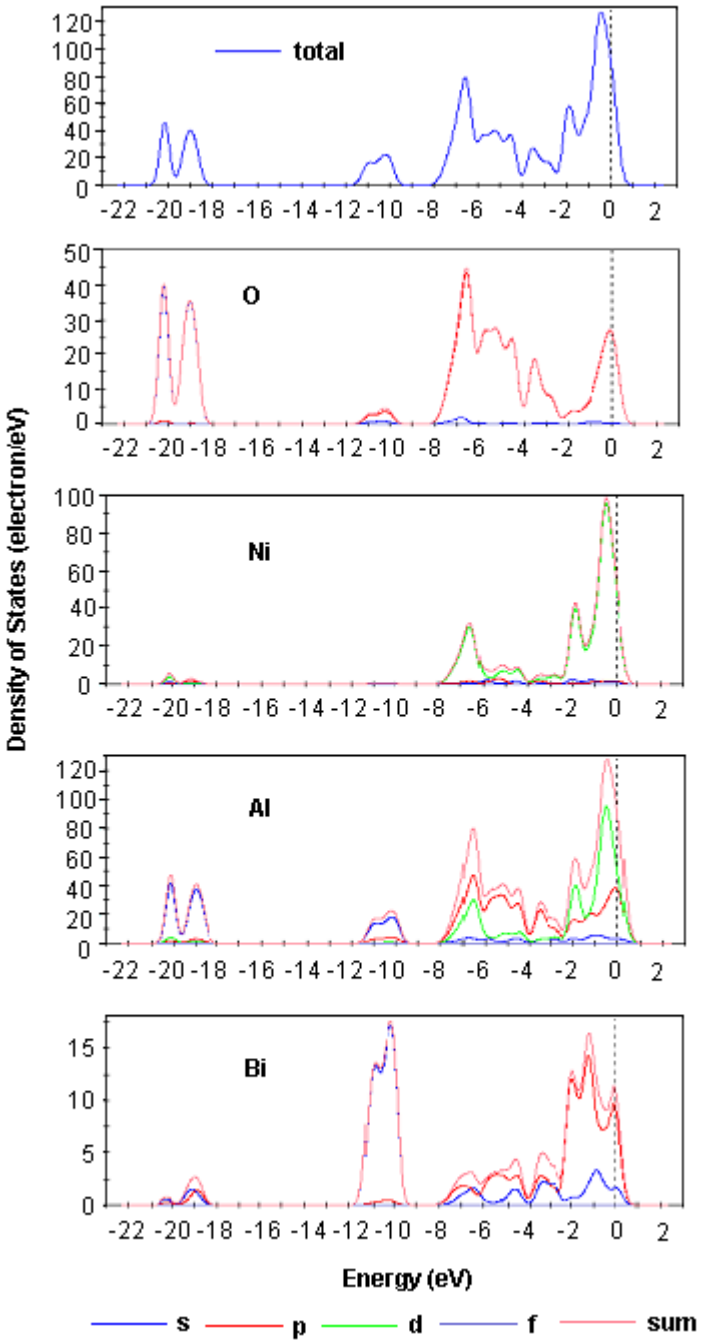

Fig. 6.Total and partial density of states of the elements O, Ni, Al, and Bi in sample $Bi_{11}Al_3Ni_7O_{28}$(A4: x= 0.75)

With the incorporation of Al^{3+} ions partially in place of Ni^{2+} in the same Wycoff sites, and the additional Bi^{3+} ions in different Wycoff sites in A2-A4, due to the absence of valence Al d orbitals and with no high energy Bi orbitals above the Fermi level, the band gap narrows

down indicating the conduction band (CB) composed predominantly of Ni e_g orbitals. This is clearly observed in the density of states plots for the samples A2-A4 where the bands ~ 1.0 eV to 2.0 eV as observed in A1 is smeared out. This results further show that the transition of semiconductor-like as in A1 to metallic character with the Ni d band predominantly crossing the Fermi level and with no high-energy Bi band present, in A2-A4 with the partial replacement of Ni^{2+} ions by Al^{3+} ions atoms in the lattice. The band in the range -11.5 to –8.5 eV is predominantly due to Bi 4f bands and Al 2s bands, and the band in the range -20.5 to -18.0 eV consists of O 2s band (Li et al., 2006).

4. CONCLUSION

Single phase composite oxides with cubic unit cell in $Bi_{2+x}Al_xNi_{4-3x}O_{7+\delta}$ (A1-A4: x = 0, 0.25, 0.50, 0.75) system is obtained by sol-gel method via nitrate-citrate route. Unit cell parameters in A1-A4 are: a = 10.2678, 10.1266, 10.1160, 10.1163 Å; Z= 4 and space group Pm3n. The average crystallite sizes in A1-A4 determined by Scherrer's relation are found to be in the range ~ 42-61 nm. DTA/TG results show no phase transitions in the range 25-800 ºC. The EDX show stoichiometry close to nominal in the samples. Rietveld refinement of the unit cell structure developed in space group Pm3n shows the appreciably lowered agreement factors R_p, R_{wp} and R_{exp} for all the samples. Electron density contour on (010) plane shows the density of Ni and O atoms in the plane as per structure. DFT calculations on the crystal of structure of A1-A4 for band structure and DOS show the valence band (VB) located at -8.0 to ~ 0.0 eV (Fermi level) predominantly comprised of O 2p orbitals overlapping with in-phase with Ni t_{2g}, and the Bi 6s orbitals to form Ni-O-Bi bonds, and O 2p orbitals overlapping with Ni t_{2g} or Bi 6s forming O-Ni-O or Bi-O-Bi covalent bonds with partial ionic character. The conduction band (CB) is predominantly composed of Ni e_g orbitals, which narrows down with complete smearing of ~ 2.0 to 3.0 eV CB as in A1 in A2-A4 due to the absence of Al^{3+} d orbitals. This result shows the transition of semiconductor-like as in A1 to metallic character with the Ni e_g band predominantly crossing the Fermi level, in A2-A4.

ACKNOWLEDGMENT

The authors thank Dr. M. M. Balakrishnarajan, for help with the Materials Studio software.

REFERENCES

Carjaval, J.R. (1990). FULLPROF program, Rietveld Pattern Matching Analysis of Powder Patterns, ILL, Grenoble.

Clark, S.J., Segall, M.D., Pickard, C.J., Hasnip, P.J., Probert, M.I.J., Refson, K., Payne, M.C. (2005). First principles methods using CASTEP. Z. Kristallogr., 220(5-6), 567-570.

Ghorai, T.K., Dhak, D., Dalai, S., Pramanik, P. (2008). Preparation and photocatalytic activity of nano-sized nickel molybdate ($NiMoO_4$) doped bismuth titanate ($Bi_2Ti_4O_{11}$) (NMBT) composite. J. Alloys and Compounds, 463, 390-397.

Hamman, D.R., Schlüter, M., Chiang, C. (1979). Norm-Conserving Pseudopotentials. Phys. Rev. Letts., 43, 1494–1497.

Hugel, J., Carabatos, C. (1983). Band structure and optical properties of NiO: I. Band structure Calculations. J. Phys. C: Solid State Phys., 16, 6713-6721.

Komarneni, S., Breval, E., Roy, R. (1986). Characterization of di-phasic nanoscale composites derived from xerogels. J. Mat. Sci., 21, 737-743.

Klug, H.P., Alexander, L.E. (1997). X-ray Diffraction procedures for polycrystalline and amorphous Materials, 2nd ed. John Wiley & Sons, New York, p. 966.

Li, D., Zheng, J., Zou, Z. (2006). Band structure and photocatalytic properties of perovskite-type compound Ca_2NiWO_6 for water splitting. J. Phys. Chem. Solids, 67, 801–806.

McCusker, L.B., Dreele, R.B.V., Cox, D.E., Louër, D., Scardi, P. (1999). Rietveld refinement guidelines. J. Appl. Cryst., (1999), 32, 36-50.

Morin, F.J. (1954). Electrical Properties of NiO. Phys. Rev., B 93(6), 1199-1204.

Perdew, J.P., Burke, K., Ernzerhof, M. (1996). Generalized Gradient Approximation Made Simple. Phys. Rev. Lett., 77, 3865–3868.

Payne, M.C., Teter, M.P., Allan, D.C., Arias, T.A., Joannopoulos, J.D. (1992). Iterative minimization techniques for *ab initio* total energy calculations:molecular dynamics and conjugate gradients. Rev. Mod. Phys., 64, 1045-1097.

Roy, R.A., Roy, R. (1984). Diphasic xerogels: I. Ceramic-metal composites. Mater. Res. Bull., 19, 169-177.

Segall, M.D., Lindan, P.L.D., Probert, M.I.J., Pickard, C.J., Hasnip, P.J., Clark, S.J., Payne, M.C. (2002a). Materials Studio CASTEP, version 2.2.

Segall, M.D., Lindan, P.L.D., Probert, M.I.J., Pickard, C.J., Hasnip, P.J., Clark, S.J., Payne, M.C. (2002b). First-principles simulation: ideas, illustrations and the CASTEP code. J. Phys.: Cond. Matt., 14, 2717-2744.

Wei, H., Liang, J.J., Sun, B.Z., Zheng, Q., Sun, X.F., Peng, P., Dargusch, M.S., Yao, X. (2010). Site preference of Ru in NiAl and valence band structure of NiAl containing Ru:
First-principles study and photoelectron spectrum. Philos. Mag. Letts., iFirst, 1–8.

Zhou, J., Zou, Z., Ray, A.K., Zhao, X.S. (2007). Preparation and Characterization of Polycrystalline Bismuth Titanate $Bi_{12}TiO_{20}$ and Its Photocatalytic Properties under Visible Light Irradiation. Ind. Eng. Chem. Res., 46, 745-749.